Journal of Geophysical Research: Atmospheres

Supporting Information for

Increasing Daytime Stability Enhances Downslope Moisture Transport in the Subcanopy of an Even-aged Conifer Forest in Western Oregon, USA

S. A. Drake[1,2], D. E. Rupp[2,3], C. K. Thomas[2,4], H. J. Oldroyd[5], M. Schulze,[6] J. A. Jones[2]

[1]Department of Physics, University of Nevada, Reno, Reno, Nevada, 89557, USA.

[2]College of Earth, Ocean, and Atmospheric Sciences, Oregon State University, Corvallis, Oregon, 97331, USA.

[3]Oregon Climate Change Research Institute, College of Earth, Ocean, and Atmospheric Sciences, Oregon State University, Corvallis, Oregon, 97331, USA.

[4]Micrometeorology, University of Bayreuth, Bayreuth, Germany.

[5]Department of Civil and Environmental Engineering, University of California, Davis, Davis, California, 95616, USA.

[6]College of Forestry, Oregon State University, Corvallis, Oregon, 97331, USA.

Contents of this file

Introduction

The following supporting figures and descriptions provide detailed information on findings that are peripheral yet relevant to the main thrust of the manuscript. The drought conditions for June and September 2012 are discussed in Section S1. Section S2 shows the prevailing wind direction at Salem OR, which is NW of the HJ Andrews Experimental Forest during the experiment time frame. Sections S3 and S4 show 1-minute averages of daily pressure (S3) and short-wave insolation (S4) for low and high stability days. Section S5 pictorially represents data discussed in Section 3.8 of the manuscript.

S1. Drought conditions, June and September, 2012

Figure S1a shows the Palmer Z index, a measure of drought conditions, for the continental United States in June 2012. During this period the HJA region had very moist conditions. By September 2012 (Figure S1b) the HJA region was in severe drought conditions.

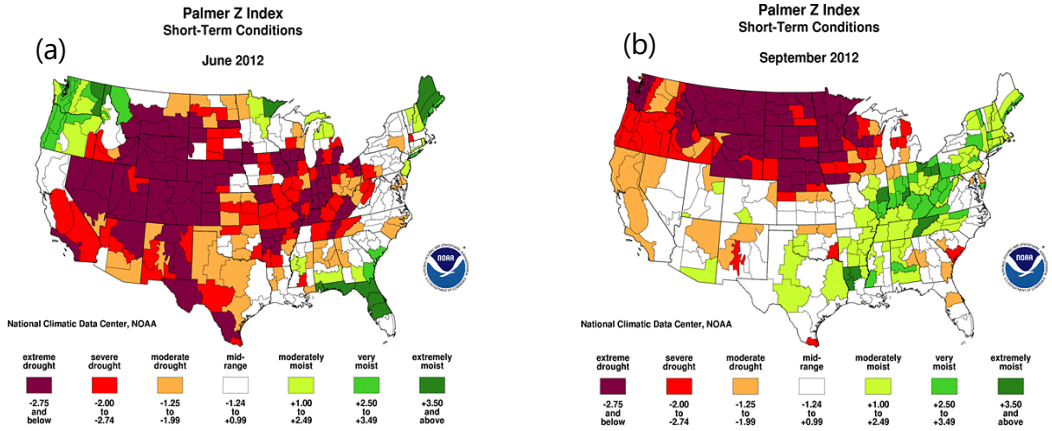

Figure S1. Palmer Z index for June 2012 (panel a) and September 2012 (panel b) for the continental US (Source NOAA NCDC).

S2. Prevailing synoptic wind direction

Figures S2 (a and b) are windroses based on 850 hPa (panel a) and 500 hPa (panel b) rawinsonde winds measured at 00Z by the Salem, Oregon (SLE) NWS office for the time period between July 19 and September 17, 2012, inclusive (data source: http://weather.uwyo.edu/). The Salem site is located approximately 104 km NW of WS1 at the HJ Andrews Experimental Forest. Mid-tropospheric winds are primarily southwesterly during this time period, which was an uncommon wind direction measured at the WS1 tower. These results in comparison with Figure 3 in the manuscript indicate that wind direction measured above and below the canopy at WS1 was due to near-field topographic airflow channeling and basin scale processes rather than synoptic forcing in addition to surface friction in the atmospheric boundary layer.

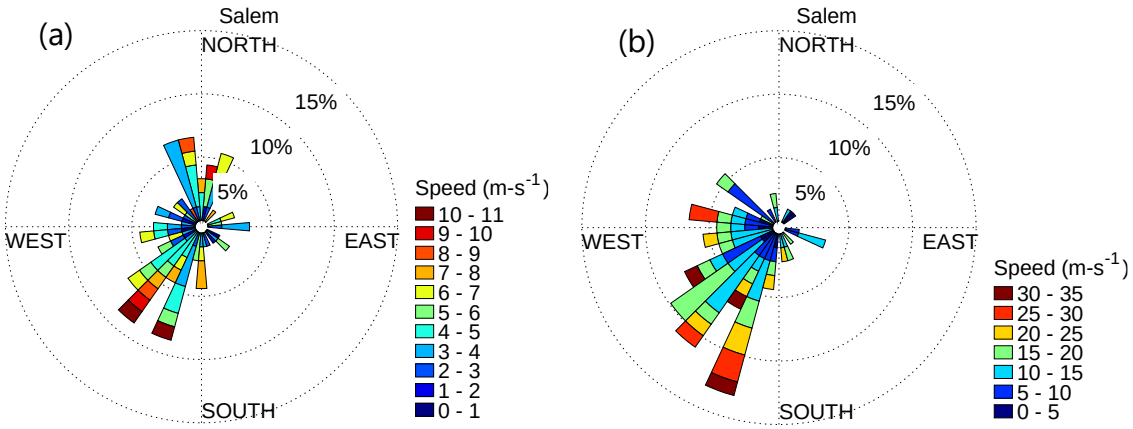

Figure S2. Windrose for 850 hPa (panel a) and 500 hPa level (panel b) derived from 00Z rawinsonde data at Salem Oregon. Timeframe for wind average is between July 19 and September 17, 2012, inclusive.

S3. Daily surface pressure range

Figure S3 shows 1-minute averaged pressure timeseries at the WS1 tower for low stability days (LS, panel a) and high stability days (HS, panel b). In both panels, the ensemble average pressure is displayed as a black line. The systematic afternoon pressure drop had greater amplitude and more coherent timing on HS days than LS days. Coherence in the pressure evolution on HS days suggests sub-canopy breeze development during a time period having a steady-state or systematically consistent pressure gradient evolution at larger-than-watershed scale. The average pressure difference between low stability (LS) and high stability (HS) days was less than 1 hPa as determined for times between 0-6 AM PST. The 0-6 AM PST time range excludes afternoon pressures, which bias HS average pressures downwards due to their larger afternoon pressure decrease. Daily standard deviations were also similar with HS days having a standard deviation of 1.6 hPa and LS days having a standard deviation of 1.2 hPa at WS1. It is important to note that plots in Figure S3 are of the pressure tendency at the WS1 tower, not the (spatial) pressure gradient.

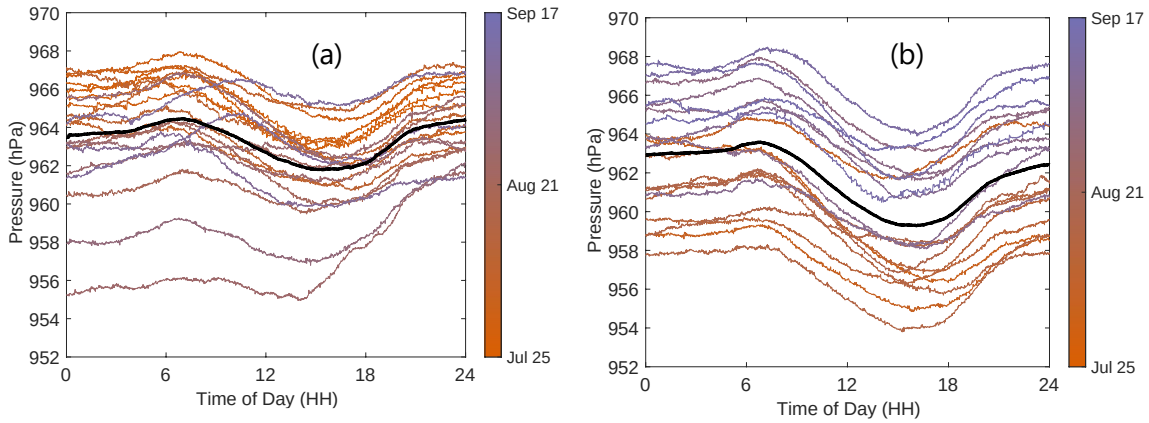

Figure S3. Daily timeseries of air pressure for LS days (panel a) and HS days (panel b) measured at the WS1 tower, color-coded by date. The black line is the ensemble average.

S4. Daily shortwave insolation

Figure S4 shows 1-minute averaged downwelling shortwave radiation measured by a pyranometer mounted at the top of the WS1 tower. Daily integrated downwelling insolation was 2% greater on LS vs. HS days or 11% greater on LS days vs. HS days when excluding overcast and partially overcast days. Although average integrated solar insolation on HS days was lower relative to LS days, HS days were consistently cloud-free or nearly so. These results suggest that the combination of weak synoptic forcing and cloudless days maximized the likelihood of canopy heating and through-canopy stability development.

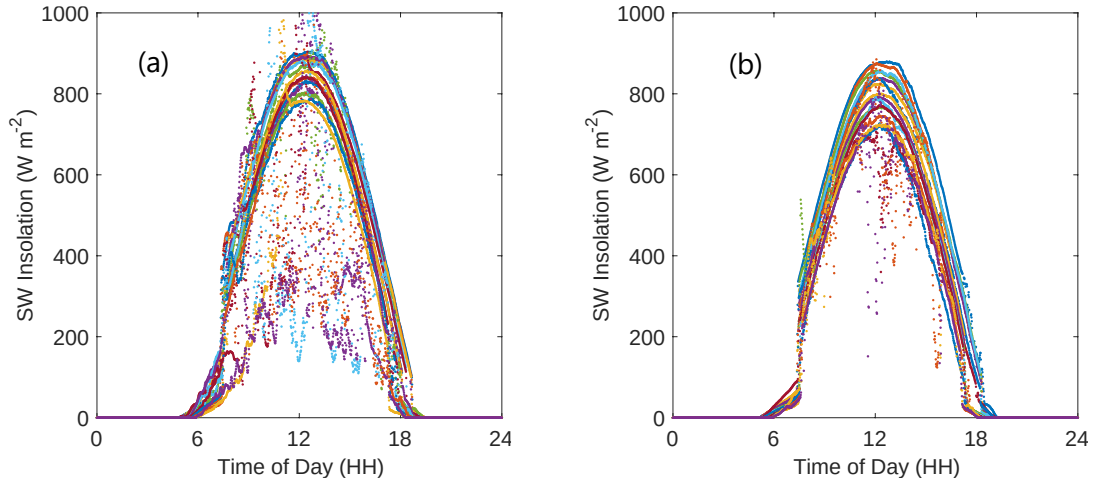

Figure S4. SW insolation for LS days (panel a) and HS days (panel b). Anomalous measurements on Aug 6 and 10, 2012 are not rendered.

S5. Sensitivity of subcanopy transport to downslope temperature gradient

Section 3.7 references a relationship between subcanopy wind speed increase as a function of the temperature difference between stations B4 and C4. Figure 5a shows this relationship. The estimated increase in downslope transport due to increasing subcanopy winds is shown in Fig 5b.

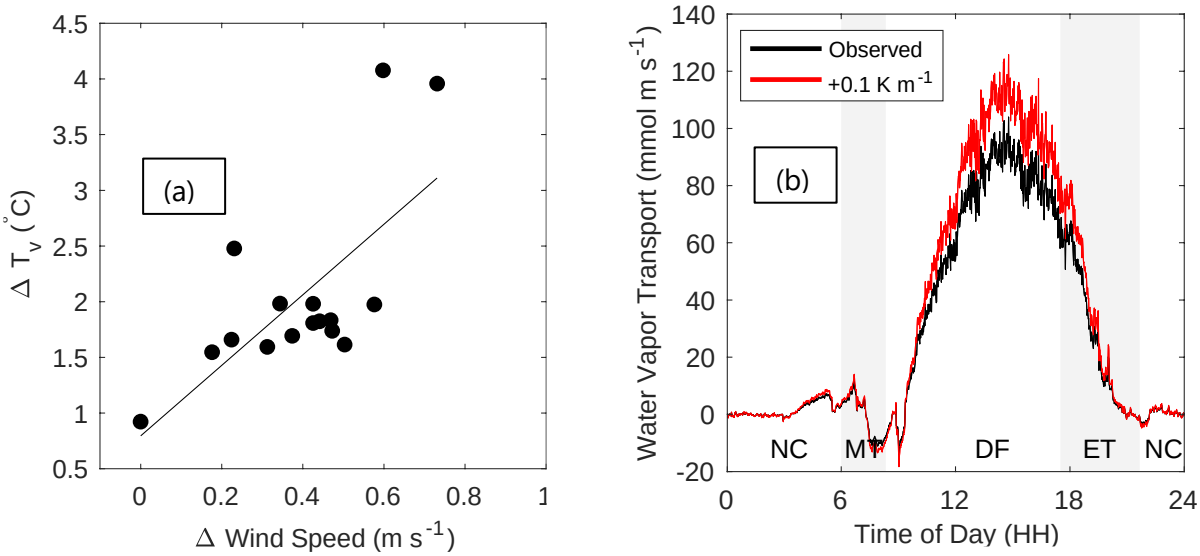

Figure S5. (a) Relationship of differences in wind speed and virtual temperature between stations B4 and C4 for HS days. (b) Composite observed water vapor transport during HS days (black) and the estimated increase in water vapor transport assuming a 0.1 K-m^{-1} static stability increase (red) due to regional climate change.